Nanoscale

Accepted Manuscript

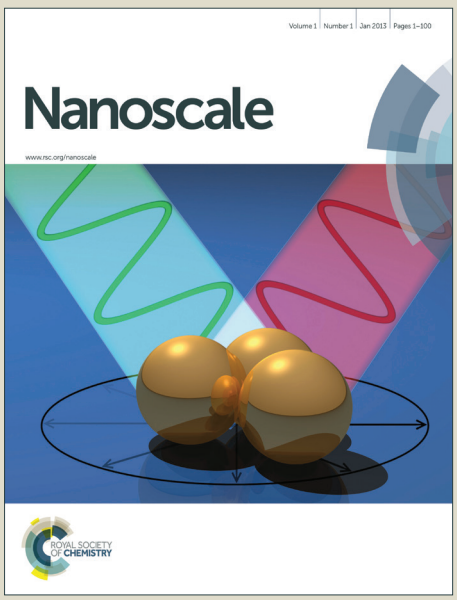

ROYAL SOCIETY OF CHEMISTRY

www.rsc.org/nanoscale

Speeding up the self-assembly of DNA nanodevice by a variety of polar solvents

Di kang[1, 2†], Ruixue Duan[1†], Yerpeng Tan[3†], Fan Hong[1], Boya Wang[1], Zhifei Chen[1], Shaofang Xu[1], Xiaoding Lou[1], Wei Wei[3*], Bernard Yurke[4] and Fan Xia[1*]

[1]School of Chemistry and Chemical Engineering, Huazhong University of Science and Technology, Wuhan, China;

[2]Department of Chemistry and Biochemistry, University of California, Santa Barbara, CA, USA;

[3]Biomolecular Science and Engineering Program, University of California, Santa Barbara, CA, USA;

[4]Department of Materials Science and Engineering, Boise State University, Boise, ID, USA

ABSTRACT:

The specific recognition and programmable assembly properties make DNA a potential material for nanodevice. However, the more intelligent the nanodevice is; the more complicated structure the nanodevice has, which limits the speed of DNA assembles. Herein, to address this problem, we investigate the performance of DNA Strand Displacement Reaction (DSDR) in the mixture of polar organic solvents and aqueous buffer, and demonstrate the organic polar solvent can speed up DNA self-assembly efficiently. Take DSDR in 20% ethanol as an example, firstly we have demonstrated DSDR is highly accelerated in the beginning of the reaction and it can complete 60% replacement reactions (160% enhancement compared with aqueous buffer) in the first 300 seconds. Secondly, we calculated that the ΔΔG of DSDR in 20% ethanol (-18.2 kcal/mol) is lower than that in pure aqueous buffer (-32.6 kcal/mol), while the activation energy is lowered by introducing ethanol. Finally, we proved that DSDR on the electrode surface can also be accelerated using this simple strategy. More importantly, to test the efficacy of this approach in the nanodevices with complicated and slow DNA self-assembly process, we apply this strategy in hybridization chain reaction (HCR) and prove the acceleration is fairly obvious in 20% ethanol, which demonstrated the feasibility of proposed strategy in DNA nanotechnology and DNA-based biosensor.

INTRODUCTION:

In vivo, DNA, carrier of genetic information, plays an extraordinary important role in life processes. In vitro, due to their specific base-pairing and the programmable sequence, DNA is employed as an ideal material for DNA nanodevice,[1-10] such as self-assembly of complex two-,[11-14] three-dimensional structures,[15-23] molecular machines,[4,5] catalytic circuits,[5,24-27] amplification reactions,[28-31] and logic gates.[24,32] With the advance of nanotechnology, DNA naodevices are developed with versatile functions. Meanwhile, however, the structures of them become complicated. The speed of DNA self-assemble, especially displacement cascading reaction,[6,10,33-37] is too slow compared to other molecular reaction such as the starch-iodide reaction, which limits its real word applications. For example, Winfree et al. had demonstrated several digital logic circuits, the most complex of which is a four-bit square-root circuit that comprises 130 DNA strands with cascading DNA hybridization and takes 10 hours to complete all of the computations.[38,39] Besides, Willner et al. developed an attractive biosensor for DNA, which also takes at least 10 hours to complete.[40] In view of their fascinating results, accelerating the cascading DNA hybridization is of interest since it would enable great improvement in DNA-based biocomputings and biosensors. More importantly, accelerating the DNA hybridization may enhance the accuracy of DNA nanotechnology because the longer hybridization time may lead to higher non-specific signals. Although several methods have been suggested to achieve this,[27,33,36,37,41-44] they mainly focused on the length and binding strength of toehold sequences, which making the experimental design complicated. One challenge in this context is fabricating DNA nanodevices which can be quickly assembled in response to external stimuli.

Herein, using the mixture of polar organic solvent and aqueous buffer which acts as reaction buffer, we overcome the above problem and speed up the processes of DNA self-assembly with many merits. Firstly, when applying the strategy in the toehold-mediated DNA strand displacement reaction (DSDR), the reaction constant is increased up to 28-fold without the need to introduce new strands or change DNA sequence. Secondly, DSDR on the surface also performed well using our strategy. Next, our approach is also potential for complicated nanodevices such as hybridization chain reaction (HCR). Finally, the compatibility of DSDR with the presence of organic solvents at relatively high concentration in buffer suggests that poor water solubility may not be an obstacle for the use of a chemical in DNA nanotechnology. We believe our strategy is promising in expanding future applications of DNA nanotechnology by improving its speed and broadening the range of its reaction environment.

RESULTS AND DISCUSSION

The performances of polar solvents on DNA self-assembly. For the proof-of-concept experiment reported herein, DSDR happened between single-strand and double-single strand DNAs was chosen as our initial system (system I) (Figure 1). To quantitatively evaluate DSDR, fluorescence spectroscopy experiments are performed by using fluorophore-labeled strands M and P. Initially, when the MP complex is intact, the fluorophore TAMRA and the quencher Iowa Black are in proximity to each other, so the fluorescence is quenched. However, when strand M is released from strand P, the quenching interaction is eliminated and the fluorescence intensity increases significantly. Results show that the MP complex can react with strand M' to form the MM' complex driven by the free energy released by hybridization of the 40 unpaired bases in the loop part (Supplementary Table S1) ($\Delta G_{MM'} - \Delta G_{MP} \approx$ -35 kcal / mol Figure 2). Before

testing the effects of organic polar solvents on DSDR, the performance of TAMRA and Iowa Black in such solutions was first studied (Supplementary Figure S1) to verify that both the fluorescence and quencher group work normally in organic polar solvents. Here, we use 20% ethanol (v/v%) as a representative system. As shown in Figure 2, DSDR in 20% ethanol solutions showed: (1) 60% replacement reactions (160% enhancement compared with aqueous buffer) in the first 300 seconds; (2) 70% displacement reactions (90% enhancement) in 660 seconds; (3) 75% displacement reactions (20% enhancement) in the range of 5000 seconds, suggesting a faster DSDR process, especially at the beginning stage of the displacement reactions.

Since DSDR is highly accelerated in the beginning of the reaction, we focused on the first 660 seconds of DSDR in the following studies. To quantitatively study the "organic polar solvent assist" effects, fluorescence spectroscopy experiments were carried out in Methanol (v/v%), Ethanol (v/v%), and Glycol (v/v%) with 3 different percentages respectively, shown in Figure 3 (Supplementary Table S4). In addition, we herein define $t_{1/2}$ as the time when DSDR has gone to 50% completion and demonstrated that $t_{1/2}$ of buffer is 2820 s, and $t_{1/2}$ of 30% methanol, ethanol, glycol, glycerin, and glucose, Acetone, and DMSO are only 315 s, 24 s, 29 s, 85 s, 160 s, 28s, and 23 s, respectively (Figure 3d).

To better understand the solvent effect on the thermodynamic properties of DSDR and the mechanism behind the DSDR acceleration induced by adding "organic polar solvent", we used ethanol as a representative example to conduct further investigations. Firstly, the melting behavior of M/M' and M/P in solutions containing differing amounts of ethanol was studied (Table 1). As shown in Figure S2, S3, S4, and S5, a higher alcohol percentage resulted in a lower melting temperature Tm (MP and MM') for 0%, 10%, 20%, and 30% ethanol, which is

consistent with previous literature reports[45] on the denaturing effects of these solutions on dsDNA. In all of the melting curves, a sharp melting transition is observed, suggesting that the multivalent and cooperative DNA binding is still functioning in the presence of the organic solvents. Then we picked the system containing 20% ethanol to measure the TM/M' and TM/P change along with M concentration while M' and P concentrations were kept constant. With a series of TM/M' and TM/P values, we are able to deduce ΔH and ΔS for M/M' and M/P in pure aqueous buffer and 20% ethanol, respectively, thus calculating ΔGM/M' and ΔGM/P at 25 ^{o}C (Supplementary Figures S6, S7, S8, S9, S10, Text S1, and Table S3). It turns out that both ΔG of M/P and M/M' increased after adding solvent which is obvious from the decrease of Tm. It is unexpected, however, that [$\Delta G_{(MM'+P)\ solvent} - \Delta G_{(MP+M')\ solvent}$=] $\Delta\Delta G_{solvent}$ (-18.2 kcal/mol) is also lower than [$\Delta G_{(MM'+P)\ buffer} - \Delta G_{(MP+M')\ buffer}$ =] $\Delta\Delta G_{buffer}$ (-32.6 kcal/mol). This suggests that adding solvent is not favorable for the displacement thermodynamically. Reaction rates of DSDR in both buffer and 20% ethanol increase with temperature (Supplementary Figures S11 and S12). The activation energies of MP strand exchange with M' can be deduced from the Arrhenius plots (Supplementary Figure S13). They are 139.2 kJ/mol (33.2 kcal/mol) and 117.3 kJ/mol (28.0 kcal/mol), respectively, in buffer and 20% ethanol. The decreased activation energy suggests that adding solvent is kinetically favorable for this DSDR process. The activation energy barrier, determined from Arrhenius plots, is thus mainly associated with the process of forming the M/P/M' complex which is lowered by adding solvents. We have already shown that adding solvent destabilizes M/P based on the decrease of Tm. This will provide more free sites for M' to attach to and thus favor the formation of M/P/M' complex. Therefore, the acceleration effect of solvent on this DSDR system may be mainly due to destabilization of M/P upon adding solvent.

The application of solar solvent-assisted accelerating reaction on solid sureface and in complicated DNA hybridization system. DSDR performance on a surface was also investigated in this research (System II). The thiol-modified strand SM is attached to a gold electrode via S-Au coupling,[46] and it hybridizes with 40 bases at one end of strand SP to form a double-strand structure as shown in Figure 4a. The DSDR of the SM/SP complex by the strand SM' is driven by more favorable free energy for SM/SM'. As shown in Figure 4a, DSDR in buffer solution is inhibited by the protective strand SP. To quantitatively evaluate DSDR, surface electro-chemistry experiments are performed by using methylene blue (MB) labeled strand SP. Initially, when the SM/SP complex stayed intact, the MB is in proximity to the gold electrode surface, so the electron transfer efficiency between the MB and the electrode is very high. However, when strand SP is released from strand SM, the electron-transfer efficiency is greatly reduced and the electrical signal of MB decreases significantly. Time-dependent surface electro-chemistry tests are carried out. When monitored by alternating current voltammetry (ACV); the displacement of SP from MB by SM' results in a decreasing faradaic current. DSDR in buffer solution only completes less than 15% during the first 600 seconds. DSDR in 20% ethanol solutions, however, completes 52% during the first 600 seconds (a 247% enhancement as shown in Figure 4b, 4c and in Supplementary Table S5). More importantly, the initial and final states differ by only 2 base pairs ($\Delta G_{MM'} - \Delta G_{MP} = 40.1 - 38.2 = 1.9$ kcal / mol). Even in DSDR with such a low $\Delta\Delta G$, ethanol can make $t_{1/2}$ almost 10 times shorter ($t_{1/2}$ for buffer is 1000 s, and $t_{1/2}$ for 20% ethanol is only 85 s in Supplementary Table S6). These results demonstrate that this solvent strategy applies not only to DSDR in solution but also to DSDR on the surface.

More importantly, to test the feasibility of the proposed strategy in the nanodevices with complicated and slow process of DNA self-assembly, hybridization chain reaction (HCR)

performances in 0%, 10%, 20%, and 30% ethanol buffer were also tested (System III). The concept of HCR was proposed by Pierce et al..[28] In HCR strategy, monomer DNAs assembled and a cascade of hybridization with nicked double helices produced in the presence of initiator strands. As showed in Figure 4e, in the presence of I, the H1, and H2 are opened, releasing fluorescence signals. Time dependent fluorescence changes are monitored. Figure 4f shows that the fluorescence signals from HCR in 10%, 20%, and 30% ethanol buffer is 1.19, 1.96, 2.16 times higher, respectively, than that from HCR in buffer solutions.

In this work we demonstrate that introducing organic polar solvent to traditional aqueous buffer is a general strategy for enhancing the reaction rates involved in DNA nanodevice. A variety of organic polar solvents consisting of alcohols, ketones, and sulfoxides were tested, and they all show an acceleration effect on DNA self-assembly. Not only the rate of DSDR in solution is increased, but also that on a surface can be accelerated using this simple strategy. More importantly, the HCR, a naodevice with complicated and slow process of DNA self-assembly, can also be efficiently accelerated by employing the mixture of ethanol and aqueous buffer. The proposed method will substantially expand the application area of DNA assembly-related technologies beyond those limited by the requirement of being compatible with pure aqueous buffer.

AUTHOR INFORMATION

Corresponding Author

xiafan@hust.edu.cn; wei.wei@mrl.ucsb.edu

Author Contributions

†These authors contributed equally. The authors declare no competing financial interests.

ACKNOWLEDGMENT

This research was supported by the National Research Fund for Fundamental Key Projects (2013CB933000), initiatory financial support from HUST, MRSEC Program of the National Science Foundation under the award No. DMR 1121053.

Supporting Information

Experimental procedures and analytical data are provided. This material is available free of charge via the Internet at http://pubs.rsc.org.

REFERENCES

(1) O. I. Wilner and I. Willner, *Chem. Rev.*, 2012, **112**, 2528-2556.

(2) N. C. Seeman, *Angew. Chem. Int. Ed.*, 1998, **37**, 3220-3238.

(3) P. E. Nielsen, M. Egholm, R. H. Berg and O. Buchardt, *Science*, 1991, **254**, 1497-1500.

(4) B. Yurke, A. J. Turberfield, A. P. Mills, F. C. Simmel and J. L. Neumann, *Nature*, 2000, **406**, 605-608.

(5) A. J. Turberfield, J. C. Mitchell, B. Yurke, A. P. Mills, M. I. Blakey and F. C. Simmel, *Phys. Rev. Lett.*, 2003, **90**, 1-4.

(6) T. Omabegho, R. Sha and N. C. Seeman, *Science*, 2009, **324**, 67-71.

(7) N. C. Seeman, *Nature*, 2003, **421**, 427-431.

(8) J. Bath and A. J. Turberfield, *Nature Nanotech.*, 2007, **2**, 275-284.

(9) S. F. J. Wickham, M. Endo, Y. Katsuda, K. Hidaka, J. Bath, H. Sugiyama and A. J. Turberfield, *Nature Nanotech.*, 2012, **7**, 166-169.

(10) P. Yin, H. M. T. Choi, C. R. Calvert and N. A. Pierce, *Nature*, 2008, **451**, 318-322.

(11) J. Sharma, Y. Ke, C. Lin, R. Chhabra, Q. Wang, J. Nangreave, Y. Liu and H. Yan, *Angew. Chem. Int. Ed.*, 2008, **47**, 5157-5159.

(12) B. Wei, M. J. Dai and P. Yin, *Nature*, 2012, **485**, 623-626.

(13) B. Ding and N. C. Seeman, *Science*, 2006, **314**, 1583-1585.

(14) M. H. S. Shyr, D. P. Wernette, P. Wiltzius, Y. Lu and P. V. Braun, *J. Am. Chem. Soc.*, 2008, **130**, 8234-8240.

(15) J. H. Chen and N. C. Seeman, *Nature*, 1991, **350**, 631-633.

(16) Y. He, T. Ye, M. Su, C. Zhang, A. E. Ribbe, W. Jiang and C. D. Mao, *Nature*, 2008, **452**, 198-202.

(17) D. Han, S. Pal, J. Nangreave, Z. Deng, Y. Liu and H. Yan, *Science*, 2011, **332**, 342-346.

(18) J. P. Zheng, J. J. Birktoft, Y. Chen, T, Wang, R. S ha, P. E. Constantinou, S. L. Ginell, C. Mao and N. C. Seeman, *Nature*, 2009, **461**, 74-77.

(19) H. Pei, N. Lu, Y. Wen, S. Song, Y. Liu, H. Yan and C. Fan, *Adv. Mater.*, 2010, **22**, 4754-4758.

(20) H. Pei, L. Liang, G. Yao, J. Li, Q. Huang and C. Fan, *Angew.Chem.*, 2012, **124**, 9154-9158.

(21) J. Li, H. Pei, B. Zhu, L. Liang, M. Wei, Y. He, N. Chen, D. Li, Q. Huang and C. Fan, *ACS nano*, 2011, **5**, 8783-8789.

(22) J. D. Flory, S. Shinde, S. Lin, Y. Liu, H. Yan, G. Ghirlanda and P. Fromme, *J. Am. Chem. Soc.*, 2013, **135**, 6985–6993.

(23) N. Lu, H. Pei, Z. Ge, C. R. Simmons, H. Yan and C. Fan, *J. Am. Chem. Soc.*, 2012, **134**, 13148-13151.

(24) G. Seelig, D. Soloveichik, D. Y. Zhang and E. Winfree, *Science*, 2006, **314**, 1585-1588.

(25) Y. Benenson, B. Gil, U. Ben-Dor, R. Adar and E. Shapiro, *Nature*, 2004, **429**, 423-429.

(26) G. Seelig, B. Yurke and E. Winfree, *J. Am. Chem. Soc.*, 2006, **128**, 12211-12220.

(27) D. Y. Zhang, A. J. Turberfield, B. Yurke and E. Winfree, *Science*, 2007, **318**, 1121-1125.

(28) R. M. Dirks and N. A. Pierce, *Proc. Natl. Acad. Sci. USA*, 2004, **101**, 15275-15278.

(29) D. Lubrich, S. J. Green and A. J. Turberfield, *J. Am. Chem. Soc.*, 2009, **131**, 2422-2423.

(30) J. Das, K. B. Cederquist, A. A. Zaragoza, P. E. Lee, E. H. Sargent and S. O. Kelley, *Nat. Chem.*, 2012, **4**, 642-648.

(31) D. Li, S. P. Song and C. H. Fan, *Acc. Chem. Res.*, 2010, **43**, 631-641.

(32) A. J. Genot, J. Bath and A. J. Turberfield, *J. Am. Chem. Soc.*, 2011, **133**, 20080-20083.

(33) A. J. Genot, D. Y. Zhang, J. Bath and A. J. Turberfield, *J. Am. Chem. Soc.*, 2011, **133**, 2177-2182.

(34) M. R. Lakin, D. Parker, L. Cardelli, M. Kwiatkowska and A. Phillips, *J. R. Soc. Interface*, 2012, **9**, 1470-1475.

(35) D. Y. Zhang and E. Winfree, *J. Am. Chem. Soc.*, 2009, **131**, 17303-17314.

(36) B. Li, Y. Jiang, Xi. Chen and A. D. Ellington, *J. Am. Chem. Soc.*, 2012, **134**, 13918–13921.

(37) D. Y. Zhang and G. Seelig, *Nat. Chem.*, 2011, **3**, 103-113.

(38) L. Qian, E. Winfree and J. Bruck, *Nature*, 2011, **475**, 368-372.

(39) L. Qian and E. Winfree, *Science*, 2011, **332**, 1196-1201.

(40) F. Wang, J. Elbaz, R. Orbach, N. Magen and I. Willner, *J. Am. Chem. Soc.*, 2011, **133**, 17149–17151.

(41) W. C. Tse and D. L. Boger, *Acc. Chem. Res.*, 2004, **37**, 61-69.

(42) D. Soloveichik, G. Seelig and E. Winfree, *Proc. Natl. Acad. Sci. USA*, 2010, 107, 5393-5398.

(43) Y. Z. Xing, Z. Q. Yang and D. S. Liu, *Angew. Chem. Int. Ed.*, 2011, **50**, 11934-11936.

(44) D. Y. Duose, R. M. Schweller, J. Zimak, A. R. Rogers, W. N. Hittelman and M. R. Diehl, *Nucleic Acids Res.*, 2012, **40**, 3289-3298.

(45) A. F. Usatyi and L. S. Shlyakhtenko, *Biopolymers*, 1974, **13**, 2435-2446.

(46) Y. Xiao, R. Y. Lai and K. W. Plaxco, *Nat. Protoc.*, 2007, **2**, 2875-2880.

Table 1. Melting temperature for MP and MM' as a function of ethanol concentration.

Category	0% Ethanol	10% Ethanol	20% Ethanol	30% Ethanol
T_{MP}	71.5 °C	67.1 °C	61.9 °C	58.1 °C
$T_{MM'}$	95.1 °C	89.2 °C	80.5 °C	77.5 °C
$T_{MM'} - T_{MP}$	23.6 °C	22.1 °C	18.6 °C	19.4 °C

Figure Caption

Figure 1. a, DSDR (MP complex) in buffer solution and 20% ethanol solution (System I). The MP complex is composed of two ssDNA strands, M and P.

Figure 2. Fluorescence spectroscopy test of DSDR in buffer solution and 20% ethanol solution in the first 5000 s (a) and in the first 660 s (b). c, The thermodynamic parameters describing DSDR after measuring the Tm values of the duplexes that formed at varying target concentrations. The slope of each fitted line is equal to the negative value of the enthalpy (-ΔH), and the intercept is equal to the entropy (ΔS). d, From ΔH and ΔS, the ΔG of DSDR in buffer and 20% ethanol is calculated.

Figure 3. Fluorescence spectroscopy test of DSDR for system I in a, methanol; b, ethanol; c, glycol with different content 0%, 10%, 20%, and 30% (v/v%) in the first 660 seconds. d, $t_{1/2}$ investigation in System I. These results indicate that polar solvents highly decrease the $t_{1/2}$.

Figure 4. a, Complex DSDR (SM/SP complex) on surface (System II). b and c are Surface electro-chemistry experiment test of DSDR in buffer solution and 20% ethanol solution for 6000 seconds and 660 seconds. d is the K constant for DSDR in buffer and 20% ethanol, respectively. e, Principle of the HCR (System III). f, Time-dependent fluorescence changes from HCR in 10%, 20%, and 30% ethanol buffer;

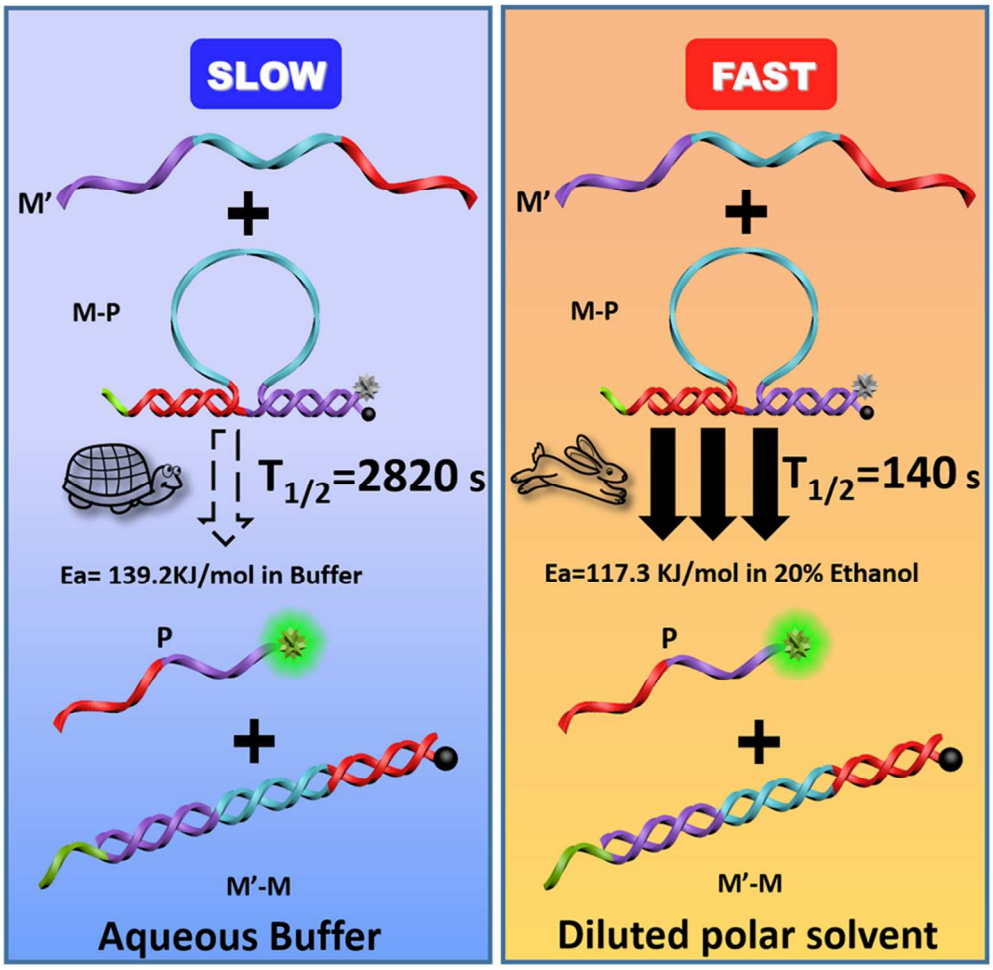

84x82mm (300 x 300 DPI)

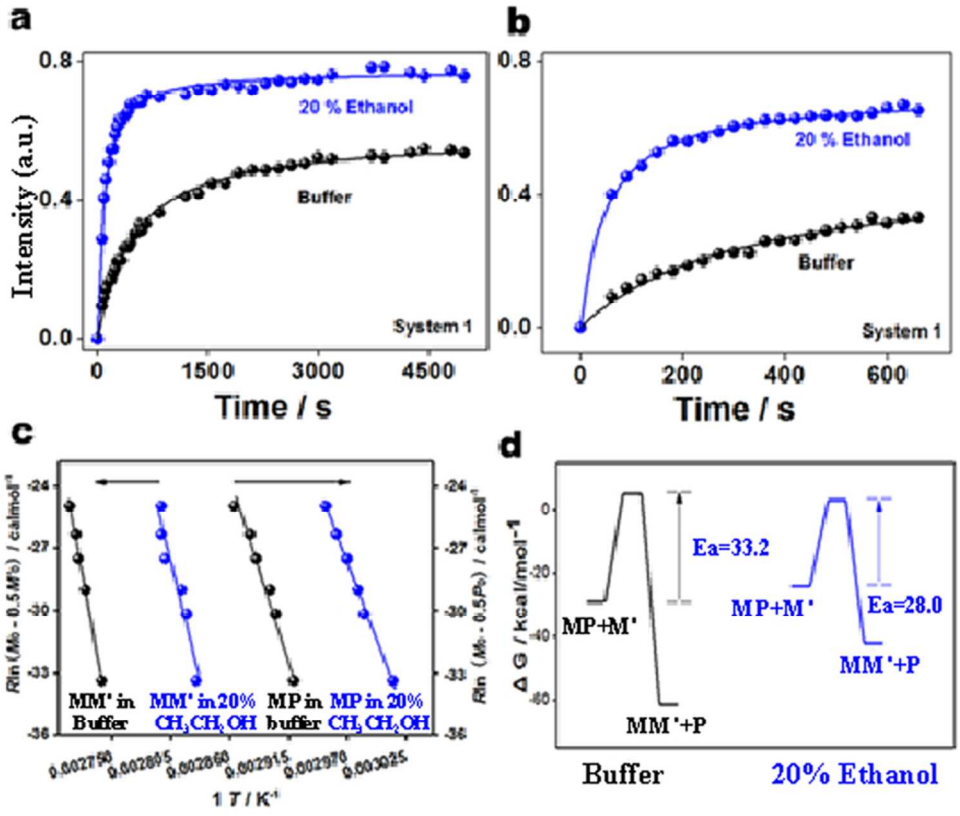

74x62mm (300 x 300 DPI)

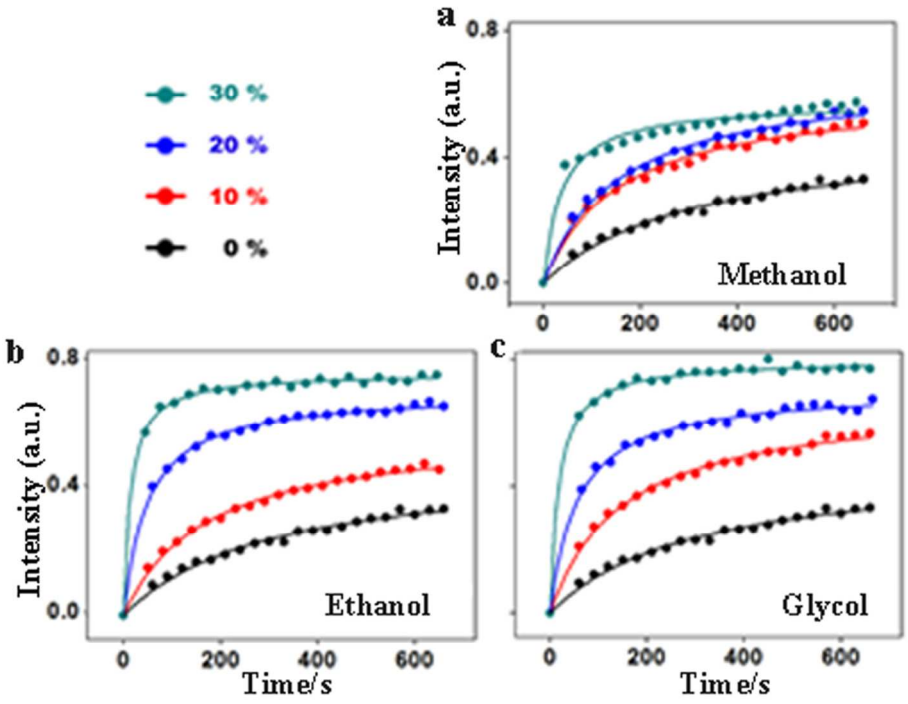

d

	10%	20%	30%
Buffer		2820 S	
Methanol	660 s	500 s	315 s
Ethanol	600 s	140 s	24 s
Glycol	450 s	140 s	29 s
Glycerin	560 s	300 s	85 s
Glucose	700 s	390 s	160 s
Acetone	652 s	58 s	28 s
DMSO	290 s	70 s	23 s

110x145mm (300 x 300 DPI)

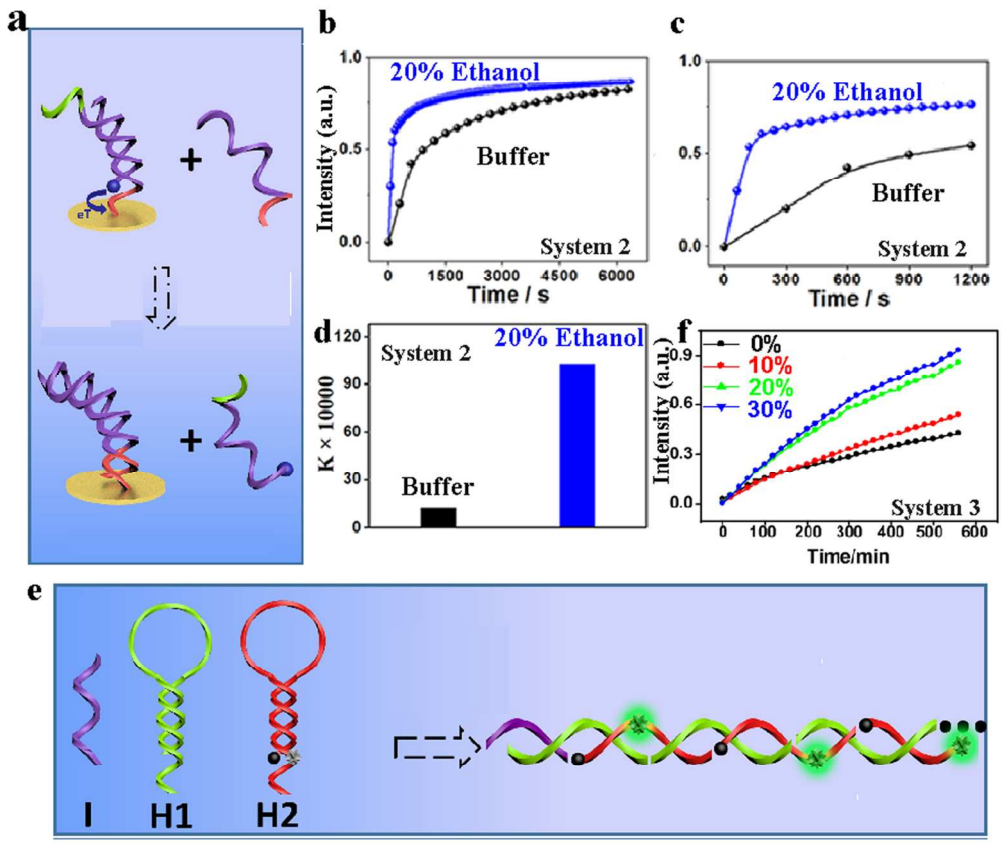

131x115mm (300 x 300 DPI)